Varying the Effective Refractive Index to Measure Optical Transport in Random Media

Sanli Faez,* P. M. Johnson, and Ad Lagendijk

FOM Institute for Atomic and Molecular Physics AMOLF, Science Park 113, 1098 XG Amsterdam, The Netherlands
(Received 6 April 2009; published 31 July 2009)

We introduce a new approach for measuring both the effective medium and the transport properties of light propagation in heterogeneous media. Our method utilizes the conceptual equivalence of frequency variation with a change in the effective index of refraction. Experimentally, we measure intensity correlations via spectrally resolved refractive index tuning, controlling the latter via changes in the ambient pressure. Our experimental results perfectly match a generalized transport theory that incorporates the effective medium and predicts a precise value for the diffusion constant. Thus, we directly confirm the applicability of the effective medium concept in strongly scattering materials.

Light propagation in multiple-scattering media is dominated by speckle, a highly irregular intensity pattern dependent upon spatial (or angular) or time (or frequency) coordinates and brought about by interference. Correlations, which are inherent properties of speckle despite the apparent irregularity, provide important information about transport parameters. In fact, the description of intensity correlations is at the heart of understanding transport theory [1]. In the past, correlations have been measured in time [2] and frequency [3] as a means of, for example, determining the diffusion constant of light.

What is often not fully appreciated is the degree to which effective medium properties are essential for determining correlation functions, and thereby transport properties. When developing a theory of transport, the effective medium is an essential building block [4]. In practice, fundamental problems arise when one attempts to access the effective medium properties of strongly scattering materials. In a turbid medium, the coherent propagation, upon which the effective medium properties are defined, decays on the scale of a few mean free paths and becomes unmeasurable in the overwhelming bath of diffuse intensity. On the other hand, the assumptions needed for developing standard effective medium models do not hold for such materials, which makes the models unapplicable. These difficulties raise the question of what exact role the effective medium plays in determining transport properties in strongly scattering materials.

In this Letter we first highlight the central role of the effective refractive index in transport theory. We then propose and measure a new correlation function that directly incorporates the effective medium approach. We validate this approach by showing the precise agreement between the theory and experimental results. This comparison requires defining a new directly measurable effective medium parameter, which we call the "tuning response," as

$$\delta \equiv \frac{1}{n_e}\frac{\partial n_e}{\partial n_h}. \qquad (1)$$

The parameter δ relates the change of the effective refractive index n_e to the changes in the refractive index n_h of one of the components, which can be easily experimentally controlled. We measure the precise value of δ with our method and use it to extract the diffusion constant. Finally, we use δ to test several standard models of the effective medium.

Our measurement method is based on controlled change of the optical path length distribution by refractive index tuning (RIT). It is the optical analogue of a class of experiments in condensed matter physics that control the elongation of electron trajectories by using magnetic field. Those experiments resulted in the observation of electronic weak localization and universal conductance fluctuations [5]. The concept of changing the path length distribution has also been exploited for diffusing wave spectroscopy [6,7], and for other types of waves in evolving media [8–10]. Given the predominance of disordered photonic media in a wide variety of fields including biology [11], advanced materials [12], solar cells [13], and modern photonics, we expect our approach to have broad cross-disciplinary application.

In standard transport theory [4], the effective refractive index shows up in the early stages where the averaged amplitude Green's function is introduced:

$$G_\omega(\mathbf{r}; n_e, l_s) = -\frac{e^{[(in_e\omega/c)-(1/2l_s)]r}}{4\pi r}, \qquad (2)$$

where l_s is the scattering mean free path. This form of the Green's function takes care of internal resonances of scatterers but does not hold in a regime of strong spatial dispersion, for example, in photonic crystals, or when the material is anisotropic. One can introduce the effective (complex-valued) wave number by $K \equiv \frac{2\pi}{\lambda_e} + i\frac{1}{2l_s}$.

We introduce a new correlation function, which is central to our measurements, defined as

$$\begin{aligned} C_{\omega,\omega+\Delta\omega}(n_e, n_e + \Delta n_e) &\equiv N[\langle I_\omega(\hat{s}; n_e)I_{\omega+\Delta\omega}(\hat{s}; n_e + \Delta n_e)\rangle \\ &\quad - \langle I_\omega(\hat{s}; n_e)\rangle \\ &\quad \times \langle I_{\omega+\Delta\omega}(\hat{s}; n_e + \Delta n_e)\rangle], \qquad (3) \end{aligned}$$
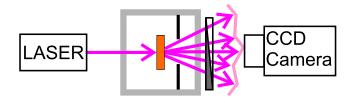
FIG. 1 (color online). The experimental setup. The sample is placed in a pressurized chamber and illuminated by a HeNe laser. A single polarization of the transmitted speckle is recorded by a CCD camera.

where $I_\omega(\hat{s})$ is the far-field specific intensity at direction $\hat{s}$ and $\langle\rangle$ denotes averaging over a narrow spread of directions. The normalization constant N is fixed by requiring $C_{\omega,\omega}(n_e, n_e) = 1$. Intensity correlations are typically classified into different contributions: $C^{(1)}$, $C^{(2)}$, and $C^{(3)}$ [1]. Their relative magnitude depends on the scattering strength of the material. We will present the closed form for the first order contribution $C^{(1)}$, which is sufficient to describe our measurements, but our argument holds for the higher-order terms as well.

The calculation of correlation function (3) for the case of $\Delta n_e = 0$ can be found in many papers and textbooks [4,14]. The actual expressions depend on the geometry. Closed forms have been presented for the case of an infinite medium [15], a semi-infinite medium [16], and a slab [3]. Yet conventional definitions of this type of correlation function have not included variations of n_e. The crucial point of the theoretical part of the present Letter is that the formulas calculated for frequency correlations can easily be generalized to the case of $\Delta n_e \neq 0$.

In our regime of consideration where

$$\frac{\Delta \text{Im} K}{\Delta \text{Re} K} \sim \frac{1}{4\pi}\left(\frac{\lambda_e}{l_s}\right)^2 \left|\frac{\Delta l_s}{\Delta \lambda_e}\right| \ll 1, \quad (4)$$

we can neglect variations of $\text{Im} K$ in the average Green's functions. As a result, the change in the average Green's function (2) is only dependent on the product $n_e\omega$. That is to say changing the frequency by $\Delta\omega$ is equivalent to changing n_e by Δn_e if $n_e\Delta\omega = \omega\Delta n_e$.

We prove that the same symmetry between frequency and effective refractive index variation holds for the intensity correlation function (3). The basic ingredients for deriving this correlation function are the average Green's function (2) and an irreducible scattering vertex [4]. We symbolically denote the irreducible scattering vertex as $U(\omega, \omega + \Delta\omega; n_e, n_e + \Delta n_e)$, and assume that it is local; thus, we have dropped the three momentum variables. Changes caused by U are compensated by those resulting from $\Delta \text{Im} K$ due to energy conservation. This cancellation holds even without considering condition (4). As a result, replacing $n_e(\omega + \Delta\omega)$ with $(n_e + \Delta n_e)(\omega + \Delta\omega)$ does not affect any algebraic step in the derivation of

$C_{\omega,\omega+\Delta\omega}(n_e, n_e)$ [14] and thus yields the generalized correlation function $C_{\omega,\omega+\Delta\omega}(n_e, n_e + \Delta n_e)$.

To take one example consider a slab of porous material, for which the host refractive index, n_h, may be tuned. The correlation is then measured as a function of n_h instead of n_e. In this case, $C^{(1)}_{\omega,\omega}(n_h, n_h + \Delta n_h)$ is given by

$$C^{(1)}_{\omega,\omega}(n_h, n_h + \Delta n_h) = \frac{\tau_\delta \Delta n_h}{\cosh\sqrt{\tau_\delta \Delta n_h} - \cos\sqrt{\tau_\delta \Delta n_h}}, \quad (5)$$

with RIT decay coefficient (generalized analogue of diffuse decay time)

$$\tau_\delta \equiv \frac{2\omega\delta L^2}{D}, \quad (6)$$

where we have used the tuning response δ defined in Eq. (1).

We apply our method to typical samples, which are representative for a large class of multiple-scattering materials. The sample dimensions are selected such that they can be characterized by both RIT and time-resolved measurements, allowing us to show the accuracy of our technique. We have used a composite material with open channels consisting of a solid backbone and a gaseous host. The refractive indices of the solid backbone and the gaseous host medium are n_s and n_h, respectively. In our measurements the index of the host is tuned by increasing the pressure of the gas.

As samples we used slabs of commercially available porous plastic air filters (XS-7744, Porex Corp.) available in different thicknesses. They are composed of sintered polyethylene spheres with a broad size distribution of 7 to 12 μm. The refractive index of the polyethylene is $n_s = 1.49$. This material has a porosity of $\phi = 0.46 \pm 0.02$ and a mean free path of $l_s = 20.6 \pm 0.2$ μm in the frequency
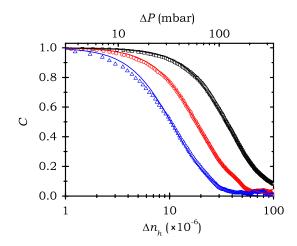

FIG. 2 (color online). RIT autocorrelation coefficient as a function of Δn_h. Data points show measurement results for 3 slabs of polyethylene filters ($L = 1$, 1.5, and 2 mm for black squares, red circles, and blue triangles, respectively). The lines show the fit to theory [Eq. (5)].

range of interest. The porosity was determined by weighing a larger sample of the same material. The mean free path was determined from total transmission measurements. These measurement also revealed a weak dependence of l_s on frequency, justifying the assumption (4).

The sample was sealed in a pressurized chamber and illuminated by a HeNe laser at 632.8 nm. Part of the transmitted speckle pattern was filtered by a linear polarizer and recorded on a 16-bit CCD camera with 10^6 pixels. The recorded image consisted of $\sim 10^4$ independent coherence areas. Gradually tuning the air pressure in the chamber changes n_h, causing the speckle pattern to evolve. This evolution allowed us to directly measure the autocorrelation coefficient defined in Eq. (3). The setup is schematically drawn in Fig. 1.

This experiment was performed on three samples. The extracted autocorrelation coefficients are plotted in Fig. 2 versus Δn_h. Each data series is fitted to the correlation function of Eq. (5) with a separate single fitting parameter, τ_δ. We see an excellent agreement between the theory and the experimental results. This agreement is an important confirmation of our theory which is built upon the concept of effective wave number in random media. This concept has never been examined so directly in strongly scattering media, simply because it was a very difficult parameter to access experimentally.

Our experimental results not only match the theoretically predicted functionality, but are quantitatively precise. We show this precision by extracting the diffusion constant from the RIT decay coefficient τ_δ and comparing it with the diffusion constant measured by a standard method. This requires the value of δ which we can measure using the symmetry relation discussed earlier in the Letter. This symmetry implies that $C_{\omega, \omega+\Delta\omega}(n_e, n_e + \Delta n_e)$ has a peak equal to one for a nonzero shift $\Delta\omega$ given by

$$(n_e + \Delta n_e)(\omega + \Delta\omega) = n_e\omega \quad \text{or} \quad \frac{\Delta\omega}{\omega} = -\frac{\Delta n_e}{n_e}. \quad (7)$$

In other words, δ can be extracted from the spectral shift of every individual speckle spot while the host index of refraction n_h is varied.

To monitor this spectral shift the experimental setup was changed. The light source was replaced by a white-light supercontinuum laser (Fianium). The CCD camera was replaced by a spectrometer, which was run in the imaging mode. The entrance slit of the spectrometer selects a transmission direction in the form of a narrow rectangle, which contains roughly 10 independent coherence areas along the slit. The beam is spectrally resolved perpendicular to the slit direction by a grating. This configuration allows us to simultaneously monitor the spectral evolution of several speckle spots while n_h is changed.

The measurement was performed on a 100-μm-thick slice of the polyethelene filter. A thin sample was necessary due to the limited resolution of our spectrometer. The intensity spectrum between 649 and 651 nm was measured while changing the pressure in the chamber from 1 to 1.5 bar in steps of 10 mbar.

RIT correlation functions at different frequencies are calculated from the measurements and plotted as a function of $\Delta\omega$ for each pressure. A collection of these plots is shown for six different pressures in the inset of Fig. 3 as typical representatives. As predicted, the peak value is
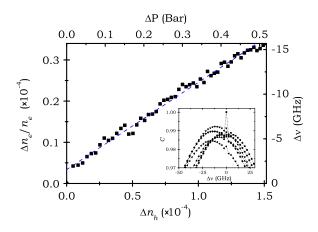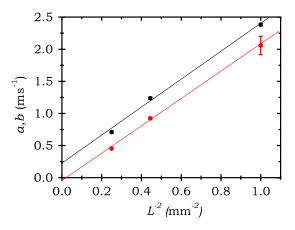
FIG. 3 (color online). Measured relative change of n_e as a function of Δn_h. The value of $\Delta n_e/n_e$ is extracted by measuring this spectral shift. The refractive index of air is calculated based on the Edlen formula [23]. Inset: The shifted cross-correlation coefficient C versus the spectral shift $\Delta\nu$ for certain pressures (from right to left: $\Delta P = 0.0$, 0.075, 0.18, 0.28, 0.37, and 0.46 bar). The peak position of each curve denotes the spectral shift, which is proportional to the relative change in the effective refractive index. The spiky feature at zero position is an artifact of the slight inhomogeneity over the detection efficiency of CCD pixels.

FIG. 4 (color online). The measurement parameters $a \equiv \frac{4\pi\nu\delta}{\tau_\delta}$ and $b \equiv \frac{1}{\pi^2\tau_d}$ are plotted versus the inverse of the thickness squared. Black squares and gray (red) dots correspond to the index tuning and time-resolved measurements, respectively. The slope of each data set is equal to the diffusion constant D measured by each specific method. The fact that the two slopes are equal proves the consistency of our index tuning method with the time-resolved measurements.

shifted and equals unity within the experimental error. Using our symmetry relation (7), the relative change of the effective refractive index is calculated and plotted as a function of Δn_h in Fig. 3. We get a value of $\delta = 0.212 \pm 0.003$ from the slope of a linear fit to the data, for this set of samples, with a remarkably high precision.

In principle, it is possible to extract the diffusion constant from each separate RIT measurement. To improve the accuracy, we plot the auxiliary parameter $a \equiv 4\pi\nu\delta/\tau_\delta$ versus L^{-2} from the three measurements presented in Fig. 2. This plot is shown in Fig. 4. The slope gives the diffusion constant $D = 2.2 \pm 0.1$ m^2/ms using Eq. (5).

Next we compare our result with the diffusion constant measured by the conventional time-resolved method. The diffuse transmission through the same samples was recorded using a time-correlated photon counting setup and a subpicosecond pulsed laser at 600 nm wavelength. The resulting temporal decay curves are presented in the supplementary information [17]. Following the guidelines of [18] and considering the response function of the detector, the diffuse decay time $\tau_d \equiv L^2/\pi^2 D$ is extracted from a fit to these measurements. These results confirm that the absorption has a negligible effect on our experiments. The diffusion constant is calculated from the slope of a linear fit of the parameter $b \equiv \frac{1}{\pi^2 \tau_d}$ vs L^{-2} (Fig. 4), $D = 2.1 \pm 0.1$ m^2/ms, which is in excellent agreement with the result from the index tuning experiment.

Our precise measurement method for measuring δ is applicable to a variety of samples, and assumes no specific effective medium model. The parameter δ can also be predicted using models of the effective medium [19–21] which are all based on long-wavelength limits.

For illustrative purposes, we present the predicted value for n_e and δ by three of the more popular effective medium theories: (i) the average permittivity [22], (ii) the Maxwell-Garnett, and (iii) the Bruggeman models. The predictions are $n_e = 1.29 \pm 0.02$, 1.25 ± 0.02, and 1.22 ± 0.02 and $\delta = 0.28 \pm 0.02$, 0.45 ± 0.03, and 0.52 ± 0.03, respectively. These predictions for δ differ from each other and from our experimental result by as much as a factor of 2. It is also worth noting that the predicted value of δ is more model dependent than n_e itself. The main reason for this discrepancy is perhaps the assumption of the long-wavelength limit, which is not reached in our experiments. Our unambiguous measurement of δ highlights the necessity of more sophisticated models of the effective medium [20].

In conclusion, we have presented a new effective medium quantity and a new transport correlation function and have shown how to precisely measure both of them by using refractive index tuning. Our measurements directly test and approve the validity of assuming an effective wave number for an inhomogeneous medium, which is very important for describing all sorts of photonic metamateri-

als. Using these two quantities one can measure several dynamic transport properties with high precision, as we have demonstrated for the lowest-order $C^{(1)}$ correlations and the diffusion constant. Measuring higher-order correlations and studying Anderson localization is a natural follow-up to our research.

*faez@amolf.nl

[1] S. Feng, C. Kane, P. A. Lee, and A. D. Stone, Phys. Rev. Lett. **61**, 834 (1988).
[2] W. Cai, B. B. Das, F. Liu, M. Zevallos, M. Lax, and R. R. Alfano, Proc. Natl. Acad. Sci. U.S.A. **93**, 13 561 (1996).
[3] A. Z. Genack, Phys. Rev. Lett. **58**, 2043 (1987).
[4] P. Sheng, *Introduction to Wave Scattering, Localization and Mesoscopic Phenomena* (Academic Press, New York, 1995).
[5] G. Bergmann, Phys. Rev. B **25**, 2937 (1982).
[6] G. Maret and P. E. Wolf, Z. Phys. B **65**, 409 (1987).
[7] D. J. Pine, D. A. Weitz, P. M. Chaikin, and E. Herbolzheimer, Phys. Rev. Lett. **60**, 1134 (1988).
[8] O. I. Lobkis and R. L. Weaver, Phys. Rev. Lett. **90**, 254302 (2003).
[9] E. Larose, J. de Rosny, L. Margerin, D. Anache, P. Gouedard, M. Campillo, and B. van Tiggelen, Phys. Rev. E **73**, 016609 (2006).
[10] R. Snieder and J. H. Page, Phys. Today **60**, No. 5, 49 (2007).
[11] A. P. Gibson, J. C. Hebden, and S. R. Arridge, Phys. Med. Biol. **50**, R1 (2005).
[12] D. R. Smith, J. B. Pendry, and M. C. K. Wiltshire, Science **305**, 788 (2004).
[13] O. L. Muskens, J. G. Rivas, R. E. Algra, E. P. A. M. Bakkers, and A. Lagendijk, Nano Lett. **8**, 2638 (2008).
[14] M. C. W. van Rossum and T. M. Nieuwenhuizen, Rev. Mod. Phys. **71**, 313 (1999).
[15] B. Shapiro, Phys. Rev. Lett. **57**, 2168 (1986).
[16] I. Freund and R. Berkovits, Phys. Rev. B **41**, 496 (1990).
[17] See EPAPS Document No. E-PRLTAO-103-034933 for supplementary material. For more information on EPAPS, see http://www.aip.org/pubservs/epaps.html.
[18] P. M. Johnson, A. Imhof, B. P. J. Bret, J. G. Rivas, and A. Lagendijk, Phys. Rev. E **68**, 016604 (2003).
[19] P. Sheng and Z. Q. Zhang, Phys. Rev. Lett. **57**, 1879 (1986).
[20] K. Busch and C. M. Soukoulis, Phys. Rev. Lett. **75**, 3442 (1995).
[21] C. F. Bohren and D. R. Huffman, *Absorption and Scattering of Light by Small Particles* (Wiley, New York, 1983).
[22] $n_e^2 = \phi n_h^2 + (1 - \phi)n_s^2$.
[23] B. Edlen, Metrologia **2**, 71 (1966).